

#### Malaysian Journal of Mathematical Sciences

Journal homepage: https://mjms.upm.edu.my



# Investigating Metric and Edge Metric Resolvability in Molecular Structures of Breast Cancer Therapeutics

Pandeeswari, E.<sup>1</sup> and Ravi Sankar, J.\* <sup>1</sup>

<sup>1</sup>Department of Mathematics, School of Advanced Sciences, Vellore Institute of Technology, Vellore - 632 014, Tamil Nadu, India

E-mail: ravisankar.j@vit.ac.in
\*Corresponding author

Received: 30 August 2024 Accepted: 15 April 2025

#### **Abstract**

Using graph theory as a conceptual framework, chemical graph theory investigates chemical structures and phenomena. Chemical graphs, with edges and vertices representing bonds and atoms, respectively, are used in chemical graph theory to represent molecular structures. The investigation of various pharmacological substances and complex molecular structures is made easier by the application of chemical graph theory. The resolvability parameter, a measure derived from graph theory, is a fundamental idea in this discipline. It requires every vertex in a structure to have a unique representation through chosen vertices, which are referred to as a metric basis, locating set, or resolving set in various scientific contexts. A key factor in describing the structural characteristics of chemical graphs is the metric dimension, which is the smallest number of vertices in the resolving set. In this work, we looked at the vertex and edge metric dimensions of the drug structures for the treatment of breast cancer, including Toremifene, Ribociclib, Tucatinib, Olaparib, and Abemaciclib and also we estimated the dimensions of the vertex and edge metrics while treating various drug structures as chemical graphs. This can make it easier to comprehend the chemical structure of different anti-breast cancer medications and create formulations more effectively.

**Keywords:** breast cancer drug molecular structure; resolving set; metric dimension; edge metric dimension.

#### 1 Introduction

Metric dimensions are a crucial characteristic for uniquely identifying vertices in molecular networks, and are the subject of current study in chemical graph theory. In order to examine complicated molecular structures like as the "M-polynomial of zigzag edge coronoid fused by starphene" molecule, studies investigate metric dimension, and mixed metric dimension [4]. In chemical graph theory, hollow coronoid structures are significant molecular graphs. In order to improve structural identification and stability analysis, this work examines their metric and fault-tolerant metric dimensions [11].

In this study [24], a unique class of molecular graphs called zigzag edge coronoid fused with starphene is studied in terms of its metric and edge metric dimension. The study investigates their structural characteristics as well as their uses in material science and nanotechnology. Crystal structures, particularly carbon's cubic forms such as diamond, are important in materials research. It investigates the mixed metric dimension, a graph theory term, to assess the cubic carbon structure's distinct features and prospective uses in material design [27]. Whereas fault-tolerant metric dimension takes resilience against errors in vertices or edges into account, metric dimension establishes the minimal number of vertices required for unique identification inside a graph. By finding groups of vertices that recognize various components in the graph, mixed metric dimension expands on these ideas and offers a greater comprehension of chemical topologies and networks [12].

Chemical graph theory also makes use of the edge version of metric dimension, as demonstrated by the study of circulant graphs with constant edge versions of metric dimension. Furthermore, linked graphs are subjected to the edge version of metric dimension, highlighting the significance of edge distances in chemical models [13]. To further clarify on their asymptotic behavior, new planar networks have been developed, such as rotationally heptagonal symmetrical graphs with up to four cords in the heptagonal structure, and their local fractional metric dimensions and upper-bound sequences analyzed [3]. With applications in chemical graph theory [19], the research investigates the zero divisor graph of commutative rings with an emphasis on graph energy and topological descriptors such as Wiener index and Zagreb indices. With algebraic graph representations, these descriptors aid in modeling molecular characteristics. Building on the work of [18], it emphasizes the interaction between algebraic structures and molecular graph theory. This study explores reverse topological indices to evaluate the chemical structures of bistar networks and corona products in the context of cheminformatics [5]. In this work, distance-based topological indices for zero divisor graphs of commutative rings are calculated, a MATLAB-based tool for their computation is presented, and their uses in algebraic structures and chemical graph theory are highlighted [9]. It offers resources for comprehending molecular characteristics and forecasting chemical reactions.

In order to help in uniquely identifying graph vertices based on distances, the study looks at the metric dimension of line graphs generated from chemical compounds [17]. This parameter is used to examine chemical structures such as fullerenes and hydrocarbons. Understanding structure-property correlations and differentiating molecular isomers are two uses for the metric dimension. The paper focuses on polycyclic aromatic hydrocarbon (PAH) networks' mixed metric dimension, which entails uniquely identifying both edges and vertices [25]. It gives insights into the structural characterisation and topological features of PAHs. The edge-based metric dimension of graphs encoding coffee chemicals is examined in this work, with an emphasis on employing resolving sets to uniquely identify edges [1]. It emphasizes uses for examining the topological uniqueness and structural characteristics of molecular structures associated with coffee. The study explores partition resolvability in graphs that depict the chemical structures of breast

cancer, with an emphasis on segmenting the graph into subsets that may be used to uniquely identify vertices [7]. This method helps in medication development by examining the topological and structural characteristics of molecules linked to breast cancer. These diverse study areas highlight how chemical graph theory is developing and how it is used in many scientific fields.

Slater [28] launched the study of standard metric dimension by posing the challenge of uniquely identifying the position of an intruder or thief in a network and locating sets as metric generators. Haray and Melter established the idea of metric dimension when they referred to the metric generators as resolving sets of a graph [6]. Subsequently, the notion of metric dimension garnered significant attention from scholars, leading to multiple publications on the subject. Examples of these studies include those on robot navigation and applications in chemistry. In addition, the following recent articles are included for the convenience of the reader [8, 26].

A few wheel graph subdivisions' metric and edge metric dimensions are calculated and explained [20]. This study aims to calculate a subset of wheel graphs' edge metric dimensions. We precisely calculate and compare the dimensions of the metric and edge metric. A graph produced by going through the spoke and cycle parts of the wheel graph. According to the results of the computations, the metric dimension issue is NP-complete [21].

Pharmaceutical chemistry, image processing, decoding complex games, robot wandering, combinatorial optimization, and other theoretical problems all involve or are at least connected to metric dimensions. Navigation in a graph framework uses landmark-based distance sensing to estimate a robot's position. This work focuses on discovering the smallest landmark set known as the metric basis and investigates the metric dimension and its computational features [10]. This study studies metric generators, which use distances to uniquely identify places in a metric space, and focuses on their importance in combinatorial optimization and graph theory [22]. Applications include estimating metric dimension, solving linked join issues, and dealing with associated computational complexity. Additionally, Nadeem et al. [15] discovered uses for metric dimensions in the polymer sector. Likewise, similar advantageous characteristics for electrical equipment may be found in [2].

In this study, we assume that atoms and the chemical bonds between them are nodes and edges, respectively, and we treat a molecular graph as a transition from a chemical structure to a graph. The findings hold great promise in the fields of pharmacology, bioinformatics, and drug research, where knowledge of molecular relationships is essential for forecasting the safety and effectiveness of medications. Additionally, the study offers a foundation for creating computational tools that simulate and model molecular interactions, which may advance the creation of specific breast cancer therapies.

In a graph, breast cancer medications can be shown as nodes, with edges denoting commonalities in structural, chemical, or functional characteristics. Drugs with similar mechanisms of action may be categorized, unique compounds can be found, and redundancy in drug libraries can be reduced by evaluating each drug's uniqueness using resolvability metrics in metric dimensions. Furthermore, comprehending therapeutic success depends heavily on IC50 values, which quantify pharmacological efficacy. Predictive models can be improved by identifying distinct pharmacological properties by combining IC50 values and chemical structure data via metric resolvability. Through the analysis of their locations within a metric-based "drug space," this method facilitates the effective identification of new medicinal substances.

Insights into Breast Cancer Drugs: The study investigates the relationship between the structural efficiency and originality of breast cancer medications and metric and edge metric dimensions. Drug-receptor interactions, biological activity prediction, and isomer separation are all

aided by molecular descriptors derived from resolvability measurements. The results show important structural elements affecting pharmacological characteristics. The development of more potent treatments for breast cancer may benefit from these revelations. The methods and mathematical terminology used in our primary research project are outlined below in Figure 1.



Figure 1: Flow chart for the computing vertex and edge metric dimension of a chemical structure.

# 2 Fundamental Concepts and Notions

**Definition 2.1.** [14] Suppose  $G_s(V(G_s), E(G_s))$  is an undirected graph of a chemical structure, where  $V(G_s)$  is the set of vertices  $G_s$  and  $E(G_s)$  is the set of edges between these vertices  $G_s$ . The distance between two vertices  $\xi_1, \xi_2 \in V(G_s)$ , written as  $d(\xi_1, \xi_2)$ , is the minimum number of edges in a path between  $\xi_1$  and  $\xi_2$ .

**Definition 2.2.** [14] Suppose  $R \subset V(G_s)$  is a subset of the vertex set, defined as  $R = \{\xi_1, \xi_2, \dots, \xi_s\}$ , and let  $\xi \in V(G_s)$ . The identification  $r(\xi \mid R)$  of a vertex  $\xi$  with respect to R is an s-ordered tuple of distances  $(d(\xi, \xi_1), d(\xi, \xi_2), \dots, d(\xi, \xi_s))$ . If each vertex from  $V(G_s)$  has a unique identification according to the ordered subset R, then this subset is called the metric basis of the graph  $G_s$ . The minimum number of elements in the subset R is called the metric dimension of  $G_s$ . Here,  $r(\xi \mid R)$  represents the position of a vertex  $\xi$  with respect to the resolving set R and for the vertex resolving set is indicated by the symbol  $R_{\xi}$ , the symbol  $R_{\xi}$  denotes the vertex resolving set; the metric dimension of a graph  $G_s$  is denoted by the symbol  $\xi$ dim $G_s$ .

**Definition 2.3.** [23, 16] A vertex  $\xi \in V(G_s)$  and an edge  $e = \xi_1 \xi_2 \in E(G_s)$ , the distance between  $\xi$  and e is defined as  $d(e, \xi) = \min\{d(\xi_1, \xi), d(\xi_2, \xi)\}$ . A vertex  $\xi \in V(G)$  distinguishes two edges  $e_1, e_2 \in E(G)$ , if  $d(\xi, e_1) \neq d(\xi, e_2)$ . A subset  $R_e$  having minimum vertices from a connected graph  $G_s$  is an edge resolving set for  $G_s$ , if any two distinct edges of  $G_s$  are distinguished by some vertex of  $R_e$ . The minimum cardinality of an edge resolving set for  $G_s$  is called the edge metric dimension. Here, the edge resolving set is denoted by the symbol  $R_e$ ; the edge metric dimension is denoted by the symbol  $edimG_s$ .

### 3 Main Results

#### 3.1 Edge metric dimensions of resolving sets for molecular graphs

Toremifene is a first generation nonsteroidal selective estrogen receptor modulator used to treat certain breast cancers. Toremifene is a selective estrogen receptor modulator (SERM) and a non-steroidal antiestrogen used to treat estrogen receptor positive breast cancer.

$$V(G_s(Te)) = \left\{ \xi_j \mid 1 \le j \le 29 \right\},$$

$$E(G_s(Te)) = \left\{ \xi_j \xi_{j+1} \mid j = 1, 2, \dots, 9, 11, \dots, 16, 18, 19, \dots, 22, 24, 25, 26, 27 \right\}$$

$$\cup \left\{ \xi_5 \xi_{10}, \xi_4 \xi_{11}, \xi_{11} \xi_{18}, \xi_{18} \xi_{23}, \xi_{17} \xi_{12}, \xi_{21} \xi_{24}, \xi_{27} \xi_{29} \right\}.$$

**Theorem 3.1.** Let  $G_s(Te)$  be a graph representing Toremifene. Then, the edge metric dimension of  $G_s(Te)$  is 4.

*Proof.* Consider the connected graph  $G_s(Te)$ , which has an edge resolving set  $R_e = \{\xi_9, \xi_{14}, \xi_{20}, \xi_{22}\}$ , as illustrated in Figure 2. The edge metric dimension of  $G_s(Te)$  is 4.

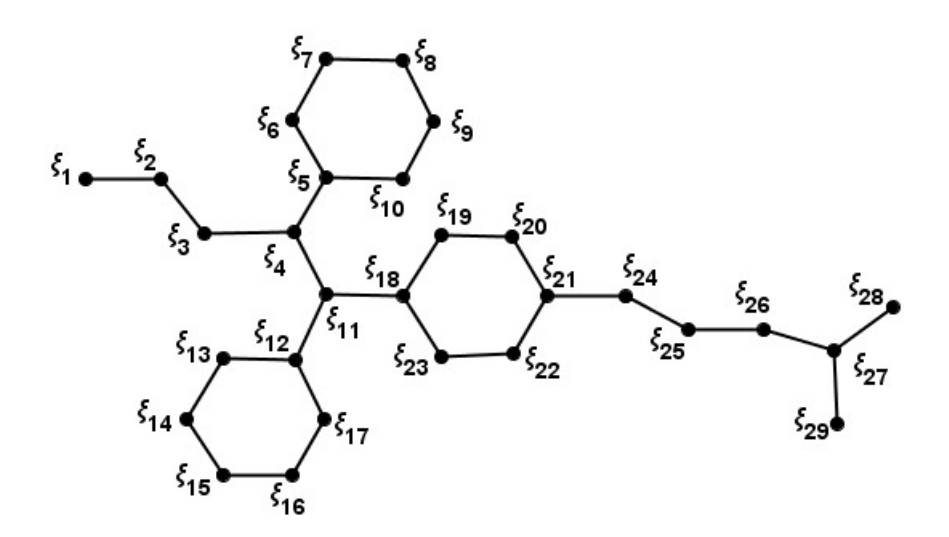


Figure 2: Molecular graph of Toremifene.

To demonstrate this, we selected an edge resolving set with a cardinality of 4 and defined it as follows,

$$r(\xi_{j}\xi_{j+1}\mid R_{e}) = \Big\{d(\xi_{j},\xi_{9}), d(\xi_{j},\xi_{14}), d(\xi_{j},\xi_{20}), d(\xi_{j},\xi_{22})\Big\}.$$

To validate this statement, we present the following representations for further discussion,

is statement, we present the following representations for further of (3(2) - j, 7 - j, 4(2) - j, 7 - j), if 
$$j = 1, 2, 3 = 3$$
 (3(2) - j, 4(2) - j, 4(2) - j, 4(2) - j), if  $j = 4, 3 = 4, 3 = 3$  (7 - j, 5(2) - j, 5(2) - j, 5(2) - j), if  $j = 5, 3 = 4, 3 = 3, 3 = 3, 3 = 2, 3 = 3, 3 = 2, 3 = 3, 3 = 2, 3, 3 = j, 33 = j,$ 

The representations for additional edges are as follows

$$r(\xi_{5}\xi_{10} \mid R_{e}) = (1, 5, 5, 5),$$

$$r(\xi_{4}\xi_{11} \mid R_{e}) = (3, 3, 3, 3),$$

$$r(\xi_{11}\xi_{18} \mid R_{e}) = (4, 3, 2, 2),$$

$$r(\xi_{12}\xi_{17} \mid R_{e}) = (5, 2, 2, 4),$$

$$r(\xi_{18}\xi_{23} \mid R_{e}) = (5, 4, 2, 1),$$

$$r(\xi_{21}\xi_{24} \mid R_{e}) = (8, 7, 1, 1),$$

$$r(\xi_{27}\xi_{29} \mid R_{e}) = (12, 11, 5, 5).$$

It is evident from each edge's unique representation with  $R_e$  that  $R_e$  is an edge resolving set of  $G_s(Te)$ , which implies,

$$\operatorname{edim}(G_s(Te)) \le 4. \tag{1}$$

Now, assume  $\operatorname{edim}(G_s(Te)) \geq 4$ . On the contrary, suppose  $\operatorname{edim}(G_s(Te)) = 3$ . We consider,

**Case 1:** Let the path  $\xi_1 \to \xi_2 \to \xi_3 \to \xi_4 \to \xi_5, \xi_{12} \to \xi_{11} \to \xi_{18}, \xi_{21} \to \xi_{24}$  be a bridge. Here,  $\xi_5\xi_6$  and  $\xi_5\xi_{10}$  are edges from  $H_1$ , while  $\xi_{12}\xi_{13}$  and  $\xi_{12}\xi_{17}$  are edges from  $H_2$ ,  $\xi_{18}\xi_{19}$  and  $\xi_{18}\xi_{23}$  are edges from  $H_3$ , showing uniform representation. The same representation will appear at the following edges if we choose an edge resolving set from  $R'_e \subset \xi(H_1)$ with a cardinality of three,

$$r(\xi_5 \xi_6 \mid R'_e) = r(\xi_5 \xi_{10} \mid R'_e).$$

As with Case 1, the resolving set fails to distinguish between these edges.

**Case 2:** The same representation will appear at the following edges if we choose an edge resolving set from  $R'_e \subset \xi(H_2)$  with a cardinality of three,

$$r(\xi_{12}\xi_{13} \mid R'_e) = r(\xi_{12}\xi_{17} \mid R'_e).$$

The same representation will appear at the following edges if we choose an edge resolving set from  $R'_e \subset \xi(H_3)$  with a cardinality of three,

$$r(\xi_{18}\xi_{19} \mid R'_{e}) = r(\xi_{18}\xi_{23} \mid R'_{e}).$$

**Case 3:** Even when considering an edge resolving set  $R'_e$  of cardinality three drawn from the union  $\xi(H_1) \cup \xi(H_2) \cup \xi(H_3)$ , the problem persists,

$$r(\xi_{5}\xi_{6} \mid R'_{e}) = r(\xi_{5}\xi_{10} \mid R'_{e}),$$
  

$$r(\xi_{12}\xi_{13} \mid R'_{e}) = r(\xi_{12}\xi_{17} \mid R'_{e}),$$
  

$$r(\xi_{18}\xi_{19} \mid R'_{e}) = r(\xi_{18}\xi_{23} \mid R'_{e}).$$

These equalities demonstrate that no edge resolving set of cardinality three can resolve all edges in  $G_s(Te)$ , as shown in Figure 3. Therefore,

$$\operatorname{edim}(G_s(Te)) \ge 4. \tag{2}$$

We conclude, based on inequalities (1) and (2), that,

$$\operatorname{edim}(G_s(Te)) = 4.$$

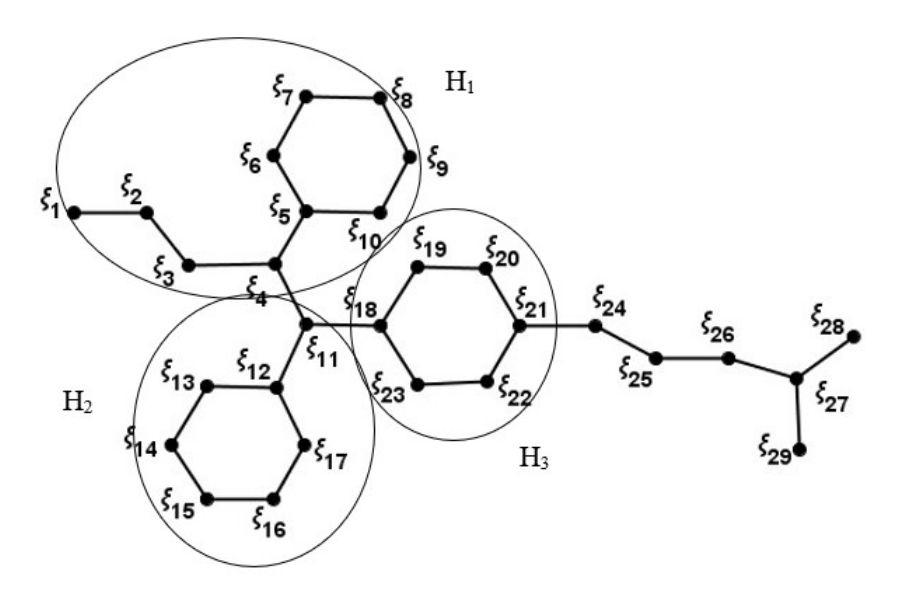


Figure 3: Partitioning of the Toremifene structure for the contrary theorem proof.

This completes the proof.

Ribociclib, a medication used in treatment, has shown great promise in treating advanced metastatic breast cancer in younger women. In addition, physicians have reported that, when

compared to standard chemotherapy, women with advanced breast cancer treated with ribociclib are able to prolong their life expectancy.

One kind of growth inhibitor for cancer is ribociclib. It specifically targets two proteins in breast cancer cells: cyclin reliant kinase 4 and cyclin dependant 6. Two proteins, CDK 4 and CDK 6, promote the growth and division of cancer cells. These proteins are blocked by ribofacilib,

$$V(G_s(Rb)) = \left\{ \xi_j \mid 1 \le j \le 32 \right\},$$

$$E(G_s(Rb)) = \left\{ \xi_j \xi_{j+1} \mid j = 1, 2, \dots, 11, 13, \dots, 21, 23, 24, 26, 29, 30, 31 \right\}$$

$$\cup \left\{ \xi_7 \xi_{12}, \xi_{18} \xi_{22}, \xi_{17} \xi_{23}, \xi_{26} \xi_{28}, \xi_{23} \xi_{29}, \xi_{14} \xi_{32}, \xi_{16} \xi_{30}, \xi_{10} \xi_{13}, \xi_{1} \xi_{6} \right\}.$$

**Theorem 3.2.** Let  $G_s(Rb)$  be a graph representing Ribociclib. Then the edge metric dimension of  $G_s(Rb)$  is 4.

*Proof.* Consider the connected graph  $G_s(Rb)$ , which has an edge resolving set  $R_e = \{\xi_2, \xi_3, \xi_9, \xi_{19}\}$ , as illustrated in Figure 4. The edge metric dimension of  $G_s(Rb)$  is 4. To demonstrate this, we selected an edge resolving set with a cardinality of 4 and defined it as follows,

$$r(\xi_j \xi_{j+1} \mid R_e) = \Big\{ d(\xi_j, \xi_2), d(\xi_j, \xi_3), d(\xi_j, \xi_9), d(\xi_j, \xi_{19}) \Big\}.$$

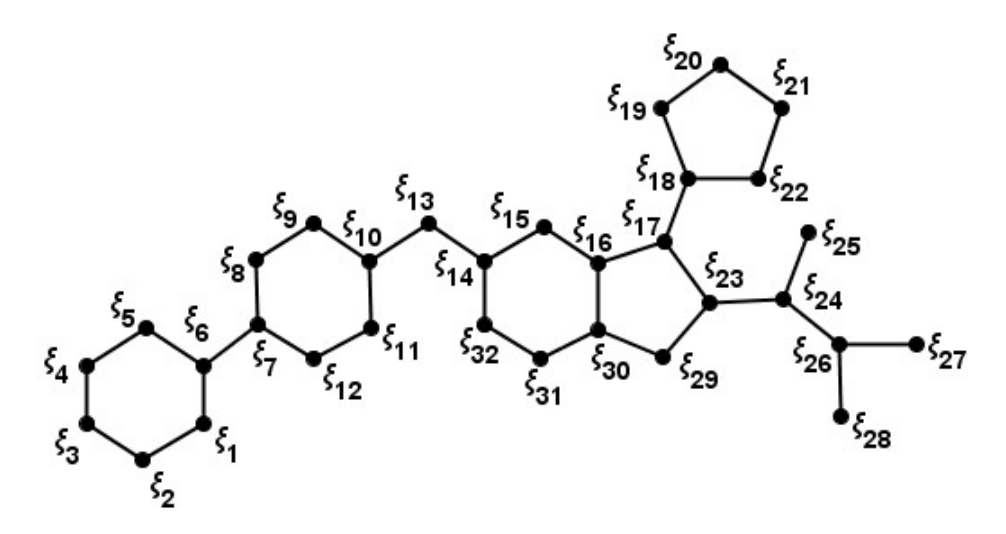


Figure 4: Molecular graph of Ribociclib.

To validate this statement, we present the following representations for further discussion,

The representations for additional edges are as follows,

$$r(\xi_{7}\xi_{12} \mid R_{e}) = (3,4,2,9), \qquad r(\xi_{1}\xi_{6} \mid R_{e}) = (1,2,3,11),$$

$$r(\xi_{18}\xi_{22} \mid R_{e}) = (12,13,7,1), \qquad r(\xi_{17}\xi_{23} \mid R_{e}) = (11,12,6,2),$$

$$r(\xi_{26}\xi_{28} \mid R_{e}) = (14,15,9,5), \qquad r(\xi_{23}\xi_{29} \mid R_{e}) = (12,13,7,3),$$

$$r(\xi_{12}\xi_{32} \mid R_{e}) = (8,9,3,5), \qquad r(\xi_{16}\xi_{30} \mid R_{e}) = (11,11,6,3),$$

$$r(\xi_{10}\xi_{13} \mid R_{e}) = (6,7,1,6), \qquad r(\xi_{24}\xi_{26} \mid R_{e}) = (13,14,8,4).$$

It is evident from each edge's unique representation with  $R_e$  that  $R_e$  is an edge resolving set of  $G_s(Rb)$ , which implies,

$$\operatorname{edim}(G_s(Rb)) \le 4. \tag{3}$$

Now, assume  $\operatorname{edim}(G_s(Rb)) \geq 4$ . On the contrary, suppose  $\operatorname{edim}(G_s(Rb)) = 3$ . We consider,

**Case 1:** Let the path  $\xi_6 \to \xi_7$ ,  $\xi_{10} \to \xi_{13} \to \xi_{14}$ ,  $\xi_{17} \to \xi_{18}$ ,  $\xi_{23} \to \xi_{24}$  be a bridges. Here,  $\xi_7 \xi_8$ and  $\xi_7\xi_{12}$  are edges from  $H_1$ , while  $\xi_{14}\xi_{15}$  and  $\xi_{14}\xi_{32}$  are edges from  $H_2$ ,  $\xi_{18}\xi_{19}$  and  $\xi_{18}\xi_{22}$  are edges from  $H_3$ , showing uniform representation. The same representation will appear at the following edges if we choose an edge resolving set from  $R'_e \subset \xi(H_1)$  with a cardinality of three,

$$r(\xi_7 \xi_8 \mid R_e') = r(\xi_7 \xi_{12} \mid R_e'),$$

as with case 1, the resolving set fails to distinguish between these edges.

**Case 2:** The same representation will appear at the following edges if we choose an edge resolving set from  $R'_e \subset \xi(H_2)$  with a cardinality of three,

$$r(\xi_{14}\xi_{15} \mid R'_e) = r(\xi_{14}\xi_{32} \mid R'_e),$$

and the same representation will appear at the following edges if we choose an edge resolving set from  $R'_e \subset \xi(H_3)$  with a cardinality of three,

$$r(\xi_{18}\xi_{19} \mid R'_e) = r(\xi_{18}\xi_{22} \mid R'_e).$$

**Case 3:** Even when considering an edge resolving set  $R'_e$  of cardinality three drawn from the union  $\xi(H_1) \cup \xi(H_2) \cup \xi(H_3)$ , the problem persists,

$$r(\xi_7 \xi_8 \mid R'_e) = r(\xi_7 \xi_{12} \mid R'_e),$$
  

$$r(\xi_{14} \xi_{15} \mid R'_e) = r(\xi_{14} \xi_{32} \mid R'_e),$$
  

$$r(\xi_{18} \xi_{19} \mid R'_e) = r(\xi_{18} \xi_{22} \mid R'_e).$$

These equalities demonstrate that no edge resolving set of cardinality three can resolve all edges in  $G_s(Rb)$ , as shown in Figure 5. Therefore,

$$\operatorname{edim}(G_s(Rb)) \ge 4. \tag{4}$$

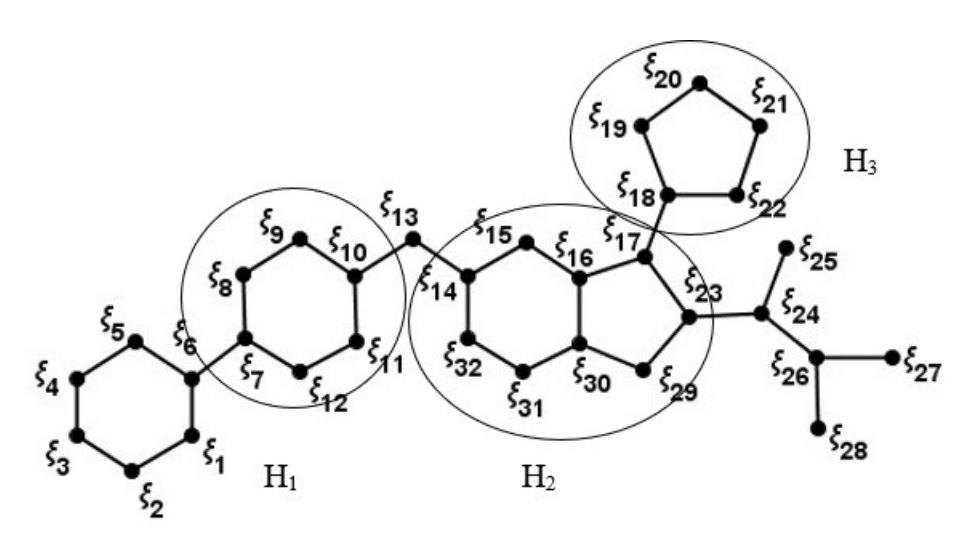


Figure 5: Partitioning of the Ribociclib structure for the contrary theorem proof.

We conclude, based on inequalities (3) and (4), that,

$$\operatorname{edim}(G_s(Rb)) = 4.$$

This completes the proof.

A kinase inhibitor medication called tucacitabine is used to treat metastatic or incurable HER-2 positive breast cancer in conjunction with trastuzumab and capecitabine. Seattle Genetics created it, and on April 17, 2020, the FDA gave it approval. For patients with metastatic breast cancer who have not reacted well to previous chemotherapy regimens, tucatinib is a potentially effective new medication,

$$V(G_s(Tb)) = \left\{ \xi_j \mid 1 \le j \le 36 \right\},$$

$$E(G_s(Tb)) = \left\{ \xi_j \xi_{j+1} \mid j = 2, 3, 4, 6, \dots, 17, 19, 20, 21, 22, 24, 25, 27, \dots, 35 \right\}$$

$$\cup \left\{ \xi_1 \xi_3, \xi_3 \xi_6, \xi_5 \xi_7, \xi_9 \xi_{18}, \xi_{12} \xi_{17}, \xi_{16} \xi_{19}, \xi_{20} \xi_{24}, \xi_{23} \xi_{27}, \xi_{28} \xi_{36}, \xi_{31} \xi_{35} \right\}.$$

**Theorem 3.3.** Let  $G_s(Tb)$  be a graph representing Tucatinib. Then the edge metric dimension of  $G_s(Tb)$  is 4.

*Proof.* Consider the connected graph  $G_s(Tb)$ , which has an edge resolving set  $R_e = \{\xi_1, \xi_2, \xi_{26}, \xi_{30}\}$ , as illustrated in Figure 6. The edge metric dimension of  $G_s(Tb)$  is 4.

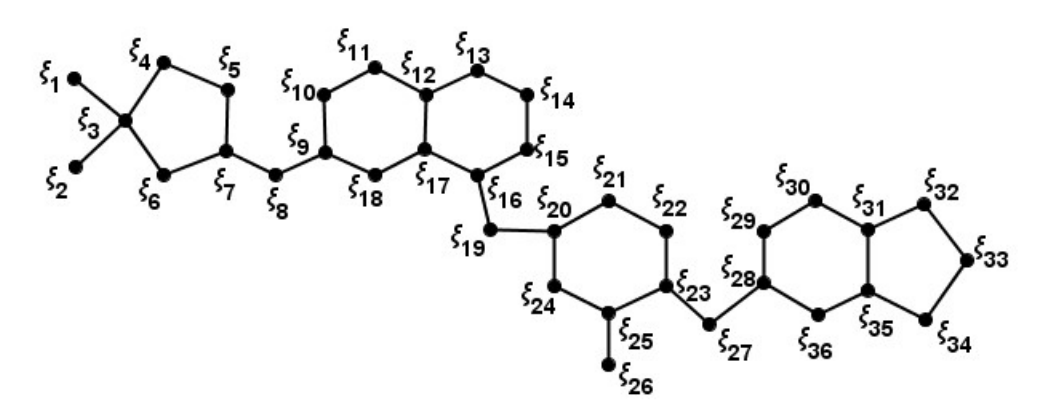


Figure 6: Molecular graph of Tucatinib.

To demonstrate this, we selected an edge resolving set with a cardinality of 4 and defined it as follows,

$$r(\xi_j \xi_{j+1} \mid R_e) = \left\{ d(\xi_j, \xi_1), d(\xi_j, \xi_2), d(\xi_j, \xi_{26}), d(\xi_j, \xi_{30}) \right\}.$$

To validate this statement, we present the following representations for further discussion,

The representations for additional edges are as follows,

$$\begin{split} r(\xi_1\xi_3 \mid R_e) &= (0,1,12,16), & r(\xi_3\xi_6 \mid R_e) &= (1,1,11,15), \\ r(\xi_5\xi_7 \mid R_e) &= (3,3,10,14), & r(\xi_9\xi_{18} \mid R_e) &= (5,5,7,11), \\ r(\xi_{12}\xi_{17} \mid R_e) &= (7,6,6,10), & r(\xi_{16}\xi_{19} \mid R_e) &= (8,8,4,8), \\ r(\xi_{20}\xi_{24} \mid R_e) &= (10,10,2,7), & r(\xi_{23}\xi_{25} \mid R_e) &= (12,12,1,4), \\ r(\xi_{23}\xi_{27} \mid R_e) &= (13,13,2,3), & r(\xi_{28}\xi_{36} \mid R_e) &= (15,15,4,2), \\ r(\xi_{31}\xi_{35} \mid R_e) &= (17,17,6,1). \end{split}$$

It is evident from each edge's unique representation with  $R_e$  that  $R_e$  is an edge resolving set of

 $G_s(Tb)$ , which implies,

$$\operatorname{edim}(G_s(Tb)) \le 4. \tag{5}$$

Now, assume edim $(G_s(Tb)) \ge 4$ . On the contrary, suppose edim $(G_s(Tb)) = 3$ . We consider,

**Case 1:** Let the path  $\xi_7 \to \xi_8 \to \xi_9$ ,  $\xi_{16} \to \xi_{19} \to \xi_{20}$ ,  $\xi_{23} \to \xi_{27} \to \xi_{28}$ ,  $\xi_{25} \to \xi_{26}$ , be a bridges. Here,  $\xi_1\xi_3$  and  $\xi_2\xi_3$  are edges from  $H_1$ , while  $\xi_{20}\xi_{21}$  and  $\xi_{20}\xi_{24}$  are edges from  $H_2$ ,  $\xi_{28}\xi_{29}$  and  $\xi_{28}\xi_{36}$  are edges from  $H_3$ , showing uniform representation.

The same representation will appear at the following edges if we choose an edge resolving set from  $R'_e \subset \xi(H_1)$  with a cardinality of three,

$$r(\xi_1 \xi_3 \mid R'_e) = r(\xi_2 \xi_3 \mid R'_e),$$

as with Case 1, the resolving set fails to distinguish between these edges.

**Case 2:** The same representation will appear at the following edges if we choose an edge resolving set from  $R'_e \subset \xi(H_2)$  with a cardinality of three,

$$r(\xi_{20}\xi_{21} \mid R'_e) = r(\xi_{20}\xi_{24} \mid R'_e),$$

and the same representation will appear at the following edges if we choose an edge resolving set from  $R'_e \subset \xi(H_3)$  with a cardinality of three,

$$r(\xi_{28}\xi_{29} \mid R'_e) = r(\xi_{28}\xi_{36} \mid R'_e).$$

**Case 3:** Even when considering an edge resolving set  $R'_e$  of cardinality three drawn from the union  $\xi(H_1) \cup \xi(H_2) \cup \xi(H_3)$ , the problem persists,

$$r(\xi_1 \xi_3 \mid R'_e) = r(\xi_2 \xi_3 \mid R'_e),$$
  

$$r(\xi_{20} \xi_{21} \mid R'_e) = r(\xi_{20} \xi_{24} \mid R'_e),$$
  

$$r(\xi_{28} \xi_{29} \mid R'_e) = r(\xi_{28} \xi_{36} \mid R'_e).$$

These equalities demonstrate that no edge resolving set of cardinality three can resolve all edges in  $G_s(Tb)$ , as shown in Figure 7. Therefore,

$$\operatorname{edim}(G_s(Tb)) \ge 4. \tag{6}$$

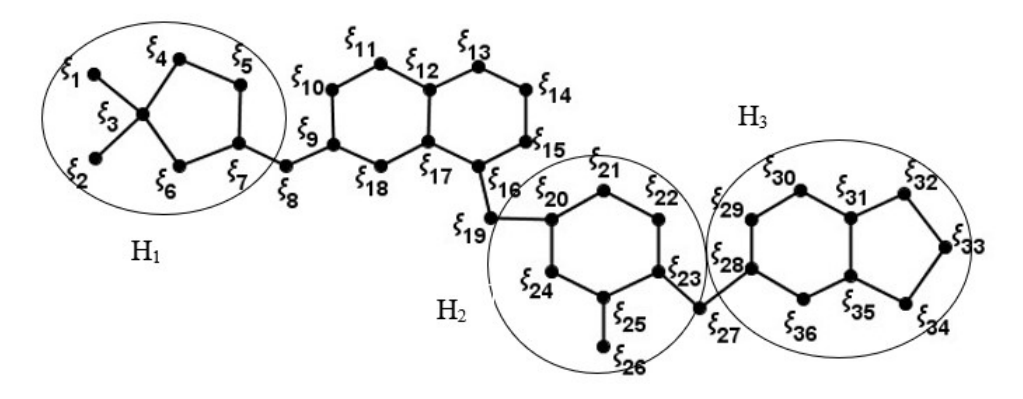


Figure 7: Partitioning of the Tucatinib structure for the contrary theorem proof.

We conclude, based on inequalities (5) and (6), that,

$$\operatorname{edim}(G_s(Tb)) = 4.$$

This completes the proof.

A PARP inhibitor is the medication used to target Olaparib. A protein called PARP aids in the self-healing process of injured cells. Olaparib halts PARP's operation. For their DNA to remain healthy, some cancer cells depend on PARP. This includes cancer cells whose BRCA genes have been altered. Thus, the cancer cells perish when olaparib prevents PARP from repairing DNA damage.

$$\begin{split} V(G_s(Ob)) &= \Big\{ \xi_j \mid 1 \leq j \leq 32 \Big\}, \\ E(G_s(Ob)) &= \Big\{ \xi_j \xi_{j+1} \mid j = 1, 2, 3, 5, 6, \dots, 10, 12, \dots, 16, 18, \dots, 24, 27, 29, 30, 31 \Big\} \\ &\qquad \qquad \cup \Big\{ \xi_1 \xi_{11}, \xi_4 \xi_6, \xi_4 \xi_{10}, \xi_9 \xi_{12}, \xi_{13} \xi_{32}, \xi_{15} \xi_{30}, \xi_{16} \xi_{18}, \xi_{18} \xi_{28}, \xi_{21} \xi_{27}, \xi_{22} \xi_{26}, \xi_{23} \xi_{25} \Big\}. \end{split}$$

**Theorem 3.4.** Let  $G_s(Ob)$  be a graph representing Olaparib. Then the edge metric dimension of  $G_s(Ob)$  is 4.

*Proof.* Consider the connected graph  $G_s(Ob)$ , which has an edge resolving set  $R_e = \{\xi_3, \xi_6, \xi_{25}, \xi_{27}\}$ , as illustrated in Figure 8. The edge metric dimension of  $G_s(Ob)$  is 4.

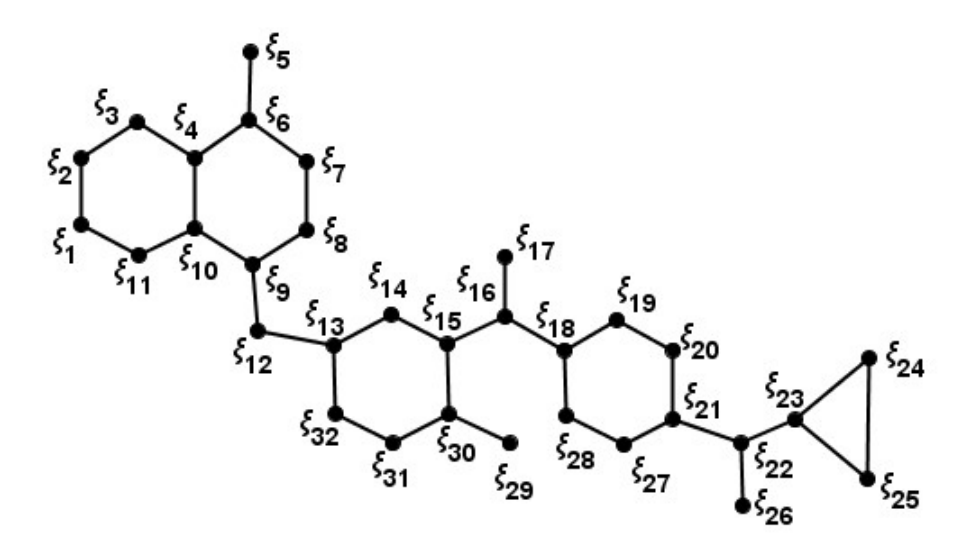


Figure 8: Molecular graph of Olaparib.

To demonstrate this, we selected an edge resolving set with a cardinality of 4 and defined it as follows,

$$r(\xi_j \xi_{j+1} \mid R_e) = \left\{ d(\xi_j, \xi_3), d(\xi_j, \xi_6), d(\xi_j, \xi_{25}), d(\xi_j, \xi_{27}) \right\}.$$

To validate this statement, we present the following representations for further discussion.

$$\begin{cases} \left(j,j+\frac{4}{2},\frac{28}{2}+j,j+\frac{20}{2}\right), & \text{if } j=1, \\ (0,4-j,7(j)+1,j+9), & \text{if } j=2, \\ (0,4-j,4(j)+2,j+7), & \text{if } j=3, \\ (7-j,5-j,5(2)+j,j+7), & \text{if } j=5, \\ (8-j,6-j,j+8,4+j), & \text{if } j=6, \\ (j-4,j-6,j+6,2+j), & \text{if } j=6, \\ (1-j,10-j,4+j,\left(\frac{j}{2}\right)+5\right), & \text{if } j=8, \\ (11-j,10-j,4+j,\left(\frac{j}{2}\right)+5\right), & \text{if } j=9, \\ (12-j,12-j,3+j,2(j)-11), & \text{if } j=10, \\ (8(2)-j,8(2)-j,j-2,j-6), & \text{if } j=13, \\ \left(j-8,\frac{j}{2}\right)-1,\left(\frac{j}{2}\right)+1,\left(\frac{j}{2}\right)-3\right), & \text{if } j=14, \\ \left(j-8,j-8,j-8,\frac{j}{5}\right), & \text{if } j=15, \\ \left(j-9,j-9,j-15,j-17\right), & \text{if } j=18, \\ \left(j-9,j-9,j-17,j-19\right), & \text{if } j=20, \\ \left(j-9,j-9,j-17,j-19\right), & \text{if } j=20, \\ \left(j-1,\frac{18}{2},j-\frac{18}{2},j-\frac{44}{2},j-\frac{40}{2}\right), & \text{if } j=23, \\ \left(j-7(3),j-7(3),j-20,j-8(3)\right), & \text{if } j=27, \\ \left(j-7(3),j-7(3),j-20,j-8(3)\right), & \text{if } j=29, \\ \left(j-23,j-22,j-21,j-5(5)\right), & \text{if } j=30, \\ \text{ntations for additional edges are as follows:} \end{cases}$$

The representations for additional edges are as follows:

$$r(\xi_{1}\xi_{11} \mid R_{e}) = (2, 3, 14, 10), \qquad (\xi_{4}\xi_{6} \mid R_{e}) = (1, 0, 15, 10), r(\xi_{4}\xi_{10} \mid R_{e}) = (1, 1, 13, 9), \qquad r(\xi_{9}\xi_{12} \mid R_{e}) = (3, 3, 11, 7), r(\xi_{13}\xi_{32} \mid R_{e}) = (5, 5, 10, 6), \qquad r(\xi_{15}\xi_{30} \mid R_{e}) = (7, 7, 8, 4), r(\xi_{16}\xi_{18} \mid R_{e}) = (8, 8, 6, 2), \qquad r(\xi_{18}\xi_{28} \mid R_{e}) = (9, 9, 6, 1), r(\xi_{21}\xi_{27} \mid R_{e}) = (11, 11, 3, 0), \qquad r(\xi_{22}\xi_{26} \mid R_{e}) = (13, 13, 2, 2), r(\xi_{23}\xi_{25} \mid R_{e}) = (14, 14, 0, 3).$$

It is evident from each edge's unique representation with  $R_e$  that  $R_e$  is an edge resolving set of

 $G_s(Ob)$ , which implies,

$$\operatorname{edim}(G_s(Ob)) \le 4. \tag{7}$$

Now, assume  $\operatorname{edim}(G_s(Ob)) \geq 4$ . On the contrary, suppose  $\operatorname{edim}(G_s(Ob)) = 3$ . We consider,

Case 1: Let the path  $\xi_9 \to \xi_{12} \to \xi_{13}$ ,  $\xi_{15} \to \xi_{16} \to \xi_{18}$ ,  $\xi_{16} \to \xi_{17}$ ,  $\xi_{21} \to \xi_{22} \to \xi_{23}$ ,  $\xi_{22} \to \xi_{26}$  be a bridges. Here,  $\xi_8\xi_9$  and  $\xi_9\xi_{10}$  are edges from  $H_1$ , while  $\xi_{20}\xi_{21}$  and  $\xi_{21}\xi_{27}$  are edges from  $H_2$ ,  $\xi_{23}\xi_{24}$  and  $\xi_{23}\xi_{25}$  are edges from  $H_3$ , showing uniform representation. The same representation will appear at the following edges if we choose an edge resolving set from  $R'_e \subset \xi(H_1)$  with a cardinality of three,

$$r(\xi_8 \xi_9 \mid R'_e) = r(\xi_9 \xi_{10} \mid R'_e),$$

as with Case 1, the resolving set fails to distinguish between these edges.

**Case 2:** The same representation will appear at the following edges if we choose an edge resolving set from  $R'_e \subset \xi(H_2)$  with a cardinality of three,

$$r(\xi_{20}\xi_{21} \mid R'_e) = r(\xi_{21}\xi_{27} \mid R'_e),$$

and the same representation will appear at the following edges if we choose an edge resolving set from  $R'_e \subset \xi(H_3)$  with a cardinality of three,

$$r(\xi_{23}\xi_{24} \mid R_e') = r(\xi_{23}\xi_{25} \mid R_e').$$

**Case 3:** Even when considering an edge resolving set  $R'_e$  of cardinality three drawn from the union  $\xi(H_1) \cup \xi(H_2) \cup \xi(H_3)$ , the problem persists,

$$r(\xi_8 \xi_9 \mid R'_e) = r(\xi_9 \xi_{10} \mid R'_e),$$
  

$$r(\xi_{20} \xi_{21} \mid R'_e) = r(\xi_{21} \xi_{27} \mid R'_e),$$
  

$$r(\xi_{23} \xi_{24} \mid R'_e) = r(\xi_{23} \xi_{25} \mid R'_e).$$

These equalities demonstrate that no edge resolving set of cardinality three can resolve all edges in  $G_s(Ob)$ , as shown in Figure 9. Therefore,

$$\operatorname{edim}(G_s(Ob)) \ge 4. \tag{8}$$

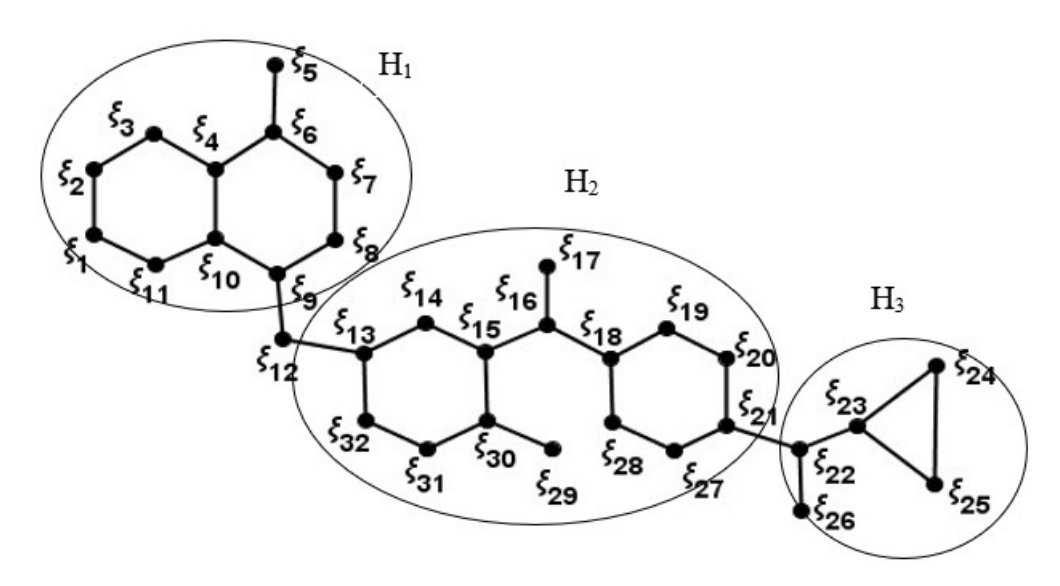


Figure 9: Partitioning of the Olaparib structure for the contrary theorem proof.

We conclude, based on inequalities (7) and (8), that,

$$edim(G_s(Ob)) = 4.$$

This completes the proof.

Breast cancer that is both HER2-negative and oestrogen receptor positive is treated with abelacicol. Bemaciclib is a member of the kinase inhibitor drug class. Abemaciclib functions by obstructing the aberrant protein that encourages the growth of cancer cells. This aids in halting or reducing the spread of cancerous cells,

$$\begin{split} V(G_s(Ab)) &= \Big\{ \xi_j \mid 1 \leq j \leq 37 \Big\}, \\ E(G_s(Ab)) &= \Big\{ \xi_j \xi_{j+1} \mid j = 1, 2, \dots, 7, 9, \dots, 14, 16, \dots, 20, 22, 24, 25, 26, 29, \dots, 32, 35, 36 \Big\} \\ &\qquad \qquad \cup \Big\{ \xi_3 \xi_8, \xi_{10} \xi_{15}, \xi_{13} \xi_{16}, \xi_{17} \xi_{23}, \xi_{20} \xi_{22}, \xi_{22} \xi_{24}, \xi_{24} \xi_{29}, \xi_{30} \xi_{28}, \xi_{26} \xi_{28}, \xi_{28} \xi_{37}, \xi_{32} \xi_{34}, \xi_{31} \xi_{36} \Big\}. \end{split}$$

**Theorem 3.5.** Let  $G_s(Ab)$  be a graph representing Abemaciclib. Then the edge metric dimension of  $G_s(Ab)$  is 4.

*Proof.* Consider the connected graph  $G_s(Ab)$ , which has an edge resolving set  $R_e = \{\xi_5, \xi_{12}, \xi_{28}, \xi_{34}\}$ , as illustrated in Figure 10. The edge metric dimension of  $G_s(Ab)$  is 4.

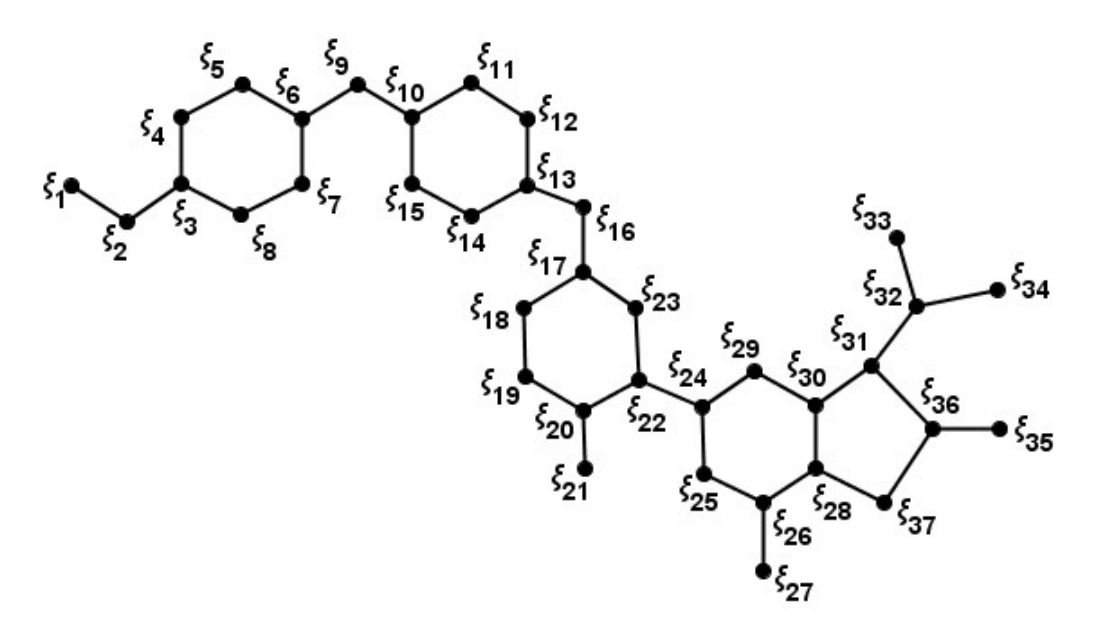


Figure 10: Molecular graph of Abemaciclib.

To demonstrate this, we selected an edge resolving set with a cardinality of 4 and defined it as follows,

$$r(\xi_j \xi_{j+1} \mid R_e) = \Big\{ d(\xi_j, \xi_5), d(\xi_j, \xi_{12}), d(\xi_j, \xi_{28}), d(\xi_j, \xi_{34}) \Big\}.$$

To validate this statement, we present the following representations for further discussion.

date this statement, we present the following representations for further discussion 
$$\begin{pmatrix} (4-j,9-j,18-j,20-j)\,, & \text{if } j=1,2,3,4,\\ (0,9-j,18-j,20-j)\,, & \text{if } j=5,\\ (7-j,10-j,19-j,21-j)\,, & \text{if } j=6,\\ (9-j,12-j,2j,2j+2)\,, & \text{if } j=7,\\ (j-7,j-7,20-j,2j-3)\,, & \text{if } j=9,\\ \left(j-7,\left(\frac{j}{5}\right)-1,j,\left(\frac{j}{2}\right)+7\right)\,, & \text{if } j=10,\\ (j-7,0,j-2,j)\,, & \text{if } j=11,\\ \left(j-7,0,j-4,\left(\frac{j}{2}\right)+4\right)\,, & \text{if } j=12,\\ \left(\frac{j}{2}-3,\left(\frac{j}{2}\right)-5,\left(\frac{j}{2}\right)+2,\left(\frac{j}{2}\right)+4\right)\,, & \text{if } j=14,\\ (j-9,j-14,5,7)\,, & \text{if } j=19,20,\\ (j-15,j-18,j-18,j-16)\,, & \text{if } j=22,\\ \left(\left(\frac{j}{2}\right)-1,\left(\frac{j}{2}\right)-6,\left(\frac{j}{12}\right),\left(\frac{j}{12}\right)+3\right)\,, & \text{if } j=24,\\ \left(\left(\frac{j}{2}\right)-1,\left(\frac{j}{2}\right)-5,\left(\frac{j}{3}\right)-1,\left(\frac{j}{13}\right)+3\right)\,, & \text{if } j=26,\\ (j-17,j-22,30-j,j-26)\,, & \text{if } j=29,\\ \left(\left(\frac{j}{3}\right)+3,\left(\frac{j}{6}\right)+3,\left(\frac{j}{6}\right)-4,\left(\frac{j}{6}\right)-3\right)\,, & \text{if } j=31,32,\\ \left(j-7(3),j-13(2),\left(\frac{j}{12}\right)-2,3\right)\,, & \text{if } j=36. \\ \text{Determinations for additional edges are as follows.}$$

The representations for additional edges are as follows,

$$r(\xi_{3}\xi_{8} \mid R_{e}) = (2, 6, 15, 19), \qquad r(\xi_{10}\xi_{15} \mid R_{e}) = (3, 2, 10, 12),$$

$$r(\xi_{13}\xi_{16} \mid R_{e}) = (6, 1, 7, 9), \qquad r(\xi_{17}\xi_{23} \mid R_{e}) = (8, 3, 5, 7),$$

$$r(\xi_{20}\xi_{22} \mid R_{e}) = (10, 5, 4, 6), \qquad r(\xi_{22}\xi_{24} \mid R_{e}) = (10, 5, 3, 5),$$

$$r(\xi_{24}\xi_{29} \mid R_{e}) = (11, 6, 2, 4), \qquad r(\xi_{30}\xi_{28} \mid R_{e}) = (13, 8, 0, 3),$$

$$r(\xi_{26}\xi_{28} \mid R_{e}) = (13, 8, 0, 4), \qquad r(\xi_{28}\xi_{37} \mid R_{e}) = (14, 9, 0, 4),$$

$$r(\xi_{31}\xi_{36} \mid R_{e}) = (14, 9, 2, 2).$$

It is evident from each edge's unique representation with  $R_e$  that  $R_e$  is an edge resolving set of  $G_s(Ab)$ , which implies,

$$\operatorname{edim}(G_s(Ab)) \le 4. \tag{9}$$

Now, assume  $\operatorname{edim}(G_s(Ab)) \geq 4$ . On the contrary, suppose  $\operatorname{edim}(G_s(Ab)) = 3$ . We consider,

Case 1: Let the path  $\xi_6 \to \xi_9 \to \xi_{10}$ ,  $\xi_{13} \to \xi_{16} \to \xi_{17}$ ,  $\xi_{22} \to \xi_{24}$ ,  $\xi_{31} \to \xi_{32}$ ,  $\xi_{36} \to \xi_{35}$  be a bridges. Here,  $\xi_5\xi_6$  and  $\xi_6\xi_7$  are edges from  $H_1$ , while  $\xi_{10}\xi_{11}$  and  $\xi_{10}\xi_{15}$  are edges from  $H_2$ ,  $\xi_{24}\xi_{25}$  and  $\xi_{24}\xi_{29}$  are edges from  $H_3$ , showing uniform representation. The same representation will appear at the following edges if we choose an edge resolving set from  $R'_e \subset \xi(H_1)$  with a cardinality of three,

$$r(\xi_5 \xi_6 \mid R'_e) = r(\xi_6 \xi_7 \mid R'_e),$$

as with Case 1, the resolving set fails to distinguish between these edges.

**Case 2:** The same representation will appear at the following edges if we choose an edge resolving set from  $R'_e \subset \xi(H_2)$  with a cardinality of three,

$$r(\xi_{10}\xi_{11} \mid R'_{e}) = r(\xi_{10}\xi_{15} \mid R'_{e}),$$

and the same representation will appear at the following edges if we choose an edge resolving set from  $R'_e \subset \xi(H_3)$  with a cardinality of three,

$$r(\xi_{24}\xi_{25} \mid R'_e) = r(\xi_{24}\xi_{29} \mid R'_e).$$

**Case 3:** Even when considering an edge resolving set  $R'_e$  of cardinality three drawn from the union  $\xi(H_1) \cup \xi(H_2) \cup \xi(H_3)$ , the problem persists,

$$r(\xi_5 \xi_6 \mid R'_e) = r(\xi_6 \xi_7 \mid R'_e),$$
  

$$r(\xi_{10} \xi_{11} \mid R'_e) = r(\xi_{10} \xi_{11} \mid R'_e),$$
  

$$r(\xi_{24} \xi_{25} \mid R'_e) = r(\xi_{24} \xi_{29} \mid R'_e).$$

These equalities demonstrate that no edge resolving set of cardinality three can resolve all edges in  $G_s(Ab)$ , as shown in Figure 11. Therefore,

$$\operatorname{edim}(G_s(Ab)) \ge 4. \tag{10}$$

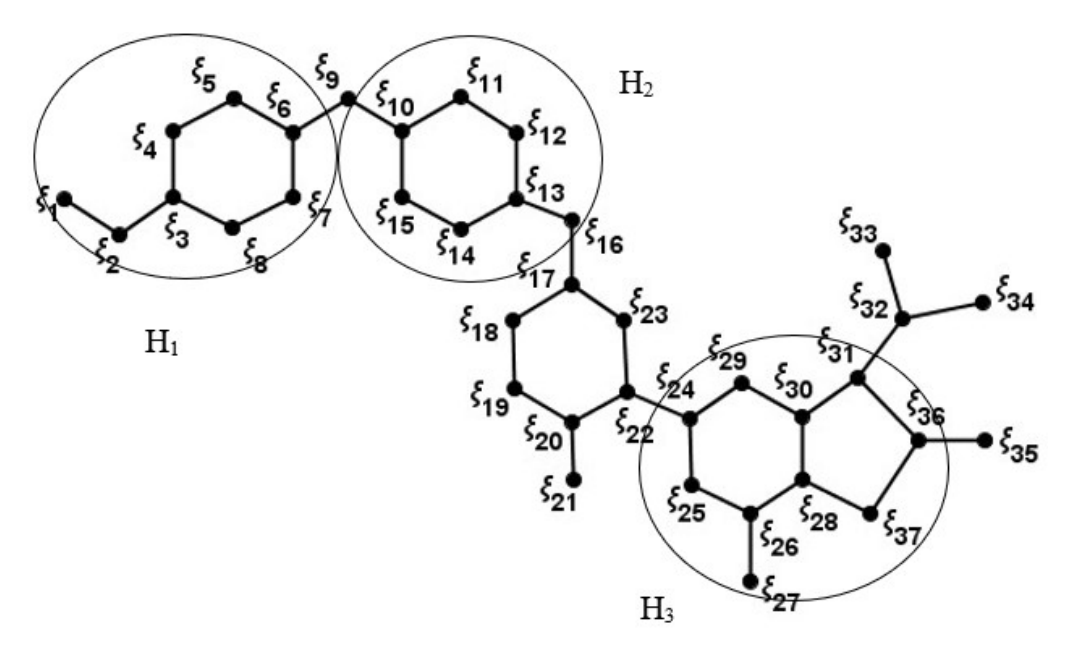


Figure 11: Partitioning of the Abemaciclib structure for the contrary theorem proof.

We conclude, based on inequalities (9) and (10), that,

$$\operatorname{edim}(G_s(Ab)) = 4.$$

This completes the proof.

## 3.2 Vertex metric dimensions of resolving set for a molecular graphs

**Theorem 3.6.** Let  $G_s(Te)$  be a graph of Toremifene. Then,  $\xi dim(G_s(Te)) = 4$ .

*Proof.* Consider the connected graph  $G_s(Te)$ , which has an vertex resolving set,

$$R_{\xi} = \left\{ \xi_7, \xi_{13}, \xi_{19}, \xi_{28} \right\},\,$$

as illustrated in Figure 2. The vertex metric dimension of  $G_s(Te)$  is 4.

To demonstrate this, we selected an vertex resolving set with a cardinality of 4 and defined it as follows,

$$r(\xi_j \mid R_{\xi}) = \{d(\xi_7), d(\xi_{13}), d(\xi_{19}), d(\xi_{28})\}.$$

To validate this statement, we present the following representations in Table 1 for further discussion,

Table 1: Resolving set of the molecular graph of Toremifene with unique vertex representations.

j	$r(\xi_{j} R_{\xi}) = \left\{ d(\xi_{7}), d(\xi_{13}), d(\xi_{19}), d(\xi_{28}) \right\}$	j	$r(\xi_{j} R_{\xi}) = \left\{ d(\xi_{7}), d(\xi_{13}), d(\xi_{19}), d(\xi_{28}) \right\}$
1, 2, 3, 4	(7-j, 7-j, 7-j, 14-j)	19	(j-13, j-15, j-19, j-12)
5	$\left(\frac{14}{2} - j, \frac{18}{2} - j, \frac{18}{2} - j, \frac{32}{2} - j\right)$	20	$\left(\left(\frac{j}{2}\right) - 3, \left(\frac{j}{2}\right) - 5, j - 19, j - 14\right)$
6,7	(7-j, j-1, j-1, j+6)	21	$\left( \left( \frac{j}{3} \right) + 1, \left( \frac{j}{3} \right) - 1, \left( \frac{j}{3} \right) - 5, \left( \frac{j}{3} \right) - 2 \right)$
8	$\left(j-7,\left(\frac{j}{2}\right)+3,\left(\frac{j}{4}\right)+5,\left(\frac{j}{2}\right)+6\right)$	22	$\left(j - \frac{30}{2}, j - \frac{34}{2}, j - \frac{38}{2}, j - \frac{32}{2}\right)$
9	$\left(j-7, \left(\frac{j}{3}\right)+3, j-3, \left(\frac{j}{3}\right)+10\right)$	23	$\left(j - \frac{34}{2}, j - \frac{38}{2}, j - \frac{42}{2}, j - \frac{32}{2}\right)$
10	$\left(j - \frac{14}{2}, j - \frac{10}{2}, j - \frac{10}{2}, j + \frac{4}{2}\right)$	24	$\left( \left( \frac{j}{4} \right) + 3, \left( \frac{j}{4} \right) + 1, \left( \frac{j}{4} \right) - 3, \left( \frac{j}{4} \right) - 2 \right)$
11	(j-7, j-9, j-9, j-2)	25	$\left( \left( \frac{j}{5} \right) + 5, \left( \frac{j}{5} \right) + 3, \left( \frac{j}{5} \right) - 1, \left( \frac{j}{5} \right) - 2 \right)$
12	$\left(j - \frac{14}{2}, j - \frac{22}{2}, j - \frac{18}{2}, j - \frac{4}{2}\right)$	26	$\left(\left(\frac{j}{2}\right) - 2, \left(\frac{j}{2}\right) - 4, \left(\frac{j}{2}\right) - 8, \left(\frac{j}{13}\right)\right)$
13, 14, 15	(j-7, j-13, j-9, j-2)	27	$\left(\left(\frac{j}{3}\right) + 3, \left(\frac{j}{3}\right) + 1, \left(\frac{j}{3}\right) - 3, 1\right)$
16	$\left(\left(\frac{j}{2}\right) - 1, \left(\frac{j}{4}\right) - 1, \left(\frac{j}{4}\right) + 1, j - 4\right)$	28	$\left(\left(\frac{j}{4}\right) + 6, \left(\frac{j}{4}\right) + 4, \left(\frac{j}{4}\right) - 5, 0\right)$
17	(j-11, j-15, j-13, j-6)	29	(j-16, j-18, j-22, j-27)
18	(j-13, j-15, j-18, j-10)		

It is evident from each vertices unique representation with  $R_{\xi}$  that  $R_{\xi}$  is an vertex resolving set of  $G_s(Te)$ , which implies,

$$\xi \dim(G_s(Te)) \le 4. \tag{11}$$

Now, assume  $\xi \dim(G_s(Te)) \ge 4$ . On the contrary, suppose  $\xi \dim(G_s(Te)) = 3$ . We consider:

**Case 1:** Let the path  $\xi_1 \to \xi_2 \to \xi_3 \to \xi_4 \to \xi_5$ ,  $\xi_{12} \to \xi_{11} \to \xi_{18}$ ,  $\xi_{21} \to \xi_{24}$ , be a bridges. Here,  $\xi_6$  and  $\xi_{10}$  are vertices from  $H_1$ , while  $\xi_{13}$  and  $\xi_{17}$  are vertices from  $H_2$ ,  $\xi_{19}$  and  $\xi_{23}$  are vertices from  $H_3$ , showing uniform representation. The same representation will appear at the following vertices if we choose an vertex resolving set from  $R'_{\xi} \subset \xi(H_1)$  with a cardinality of three,

$$r(\xi_6 \mid R'_{\xi}) = r(\xi_{10} \mid R'_{\xi}).$$

It is impossible to resolve all the vertices.

**Case 2:** The same representation will appear at the following vertices if we choose an vertex resolving set from  $R'_{\xi} \subset \xi(H_2)$  with a cardinality of three,

$$r(\xi_{13} \mid R'_{\varepsilon}) = r(\xi_{17} \mid R'_{\varepsilon}),$$

and the same representation will appear at the following vertices if we choose an vertex resolving set from  $R'_{\xi} \subset \xi(H_3)$  with a cardinality of three,

$$r(\xi_{19} \mid R'_{\xi}) = r(\xi_{23} \mid R'_{\xi}),$$

**Case 3:** Even when considering an edge resolving set  $R'_{\xi}$  of cardinality three drawn from the union  $\xi(H_1) \cup \xi(H_2) \cup \xi(H_3)$ , the problem persists,

$$r(\xi_6 \mid R'_{\xi}) = r(\xi_{10} \mid R'_{\xi}),$$
  

$$r(\xi_{13} \mid R'_{\xi}) = r(\xi_{17} \mid R'_{\xi}),$$
  

$$r(\xi_{19} \mid R'_{\xi}) = r(\xi_{23} \mid R'_{\xi}).$$

These equalities demonstrate that no vertex resolving set of cardinality three can resolve all vertices in  $G_s(Te)$ , as shown in Figure 3. Therefore,

$$\xi \dim(G_s(Te)) \ge 4. \tag{12}$$

We conclude by inequalities (11) and (12),

$$\xi \dim(G_s(Te)) = 4.$$

This completes the proof.

**Theorem 3.7.** Let  $G_s(Rb)$  be a graph of Ribociclib . Then  $\xi dim(G_s(Rb)) = 4$ .

*Proof.* Consider the connected graph  $G_s(Rb)$ , which has an vertex resolving set  $R_{\xi} = \{\xi_2, \xi_{11}, \xi_{20}, \xi_{27}\}$ , as illustrated in Figure 4. The vertex metric dimension of  $G_s(Rb)$  is 4.

To demonstrate this, we selected an vertex resolving set with a cardinality of 4 and defined it as follows,

$$r(\xi_j \mid R_{\xi}) = \Big\{ d(\xi_2), d(\xi_{11}), d(\xi_{20}), d(\xi_{27}) \Big\}.$$

To validate this statement, we present the following representations in Table 2 for further discussion,

 $r(\xi_{j}|R_{\xi}) = \left\{ d(\xi_{2}), d(\xi_{11}), d(\xi_{20}), d(\xi_{27}) \right\}$  $r(\xi_{j}|R_{\xi}) = \left\{ d(\xi_{2}), d(\xi_{11}), d(\xi_{20}), d(\xi_{27}) \right\}$ jj $\left(j-\frac{12}{2},j-\frac{22}{2},j-\frac{28}{2},j-\frac{26}{2}\right)$ (j, j+3, j+12, j+13)17 1 2 (0,7-j,16-j,17-j)18 (j-6, j-11, j-16, j-13) $\left(\frac{8}{2}-j,\frac{18}{2}-j,\frac{36}{2}-j,\frac{38}{2}-j\right)$ (j-6, j-11, j-18, j-13)3 19  $\left(j-\frac{4}{2},j+1,j(2)+2,j(3)+3\right)$  $+4, \left(\frac{j}{2}\right) - 1, 0, j - 13$ 20 4 (8-j, 9-j, 18-j, 19-j)5,6 21 (10-j, 9-j, 18-j, 19-j)7 228 (12 - j, j - 5, 18 - j, 19 - j)(j-11, j-16, j-19, j-20)23 (14 - j, j - 7, 18 - j, 19 - j)(j-11, j-16, j-19, j-22)9 24, 25(16 - j, j - 9, 18 - j, 19 - j)10 26 (j-12, j-17, j-20, j-25) $\left(\frac{j}{2}\right) + 6, \left(\frac{j}{2}\right) + 1, \left(\frac{j}{2}\right) - 2, 0$ (16-j, j-11, j-2, 21-j)11 27  $\left(16 - j, j - 11, \left(\frac{j}{2}\right) + 4, \left(\frac{j}{2}\right) + 5\right)$ 12 28 (20 - j, j - 11, 20 - j, j - 5)(j-17, j-22, j-24, j-25)13 29

Table 2: Resolving set of the molecular graph of Ribociclib with unique vertex representations.

It is evident from each vertices unique representation with  $R_{\xi}$  that  $R_{\xi}$  is an vertex resolving set of  $G_s(Rb)$ , which implies,

30

31

32

$$\xi \dim(G_s(Rb)) \le 4. \tag{13}$$

(j-19, j-24, j-25, j-25)

(j-21, j-26, j-25, j-25)

(j-23, j-28, j-25, j-25)

Now, assume  $\xi \dim(G_s(Rb)) \ge 4$ . On the contrary, suppose  $\xi \dim(G_s(Rb)) = 3$ . We consider:

 $\left(\frac{j}{2}\right) + 1, \left(\frac{j}{2}\right) - 4, \left(\frac{j}{2}\right) - 1, \left(\frac{j}{2}\right)$ 

 $(j - \frac{12}{2}, j - \frac{22}{2}, j - \frac{20}{2}, j - \frac{18}{2})$ 

 $(j - \frac{12}{2}, j - \frac{22}{2}, j - \frac{24}{2}, j - \frac{22}{2})$ 

Case 1: Let the path  $\xi_6 \to \xi_7$ ,  $\xi_{10} \to \xi_{13} \to \xi_{14}$ ,  $\xi_{17} \to \xi_{18}$ ,  $\xi_{23} \to \xi_{24}$ , be a bridges. Here,  $\xi_8$  and  $\xi_{12}$  are vertices from  $H_1$ , while  $\xi_{15}$  and  $\xi_{32}$  are vertices from  $H_2$ ,  $\xi_{19}$  and  $\xi_{22}$  are vertices from  $H_3$ , showing uniform representation. The same representation will appear at the following vertices if we choose an vertex resolving set from  $R'_{\xi} \subset \xi(H_1)$  with a cardinality of three,

$$r(\xi_8 \mid R'_{\xi}) = r(\xi_{12} \mid R'_{\xi}).$$

14

15

16

It is impossible to resolve all the vertices.

**Case 2:** The same representation will appear at the following vertices if we choose an vertex resolving set from  $R'_{\xi} \subset \xi(H_2)$  with a cardinality of three,

$$r(\xi_{15} \mid R'_{\xi}) = r(\xi_{32} \mid R'_{\xi}),$$

and the same representation will appear at the following vertices if we choose an vertex resolving set from  $R'_{\xi} \subset \xi(H_3)$  with a cardinality of three,

$$r(\xi_{19} \mid R'_{\xi}) = r(\xi_{22} \mid R'_{\xi}).$$

**Case 3:** Even when considering an edge resolving set  $R'_{\xi}$  of cardinality three drawn from the union  $\xi(H_1) \cup \xi(H_2) \cup \xi(H_3)$ , the problem persists,

$$r(\xi_8 \mid R'_{\xi}) = r(\xi_{12} \mid R'_{\xi}),$$
  

$$r(\xi_{15} \mid R'_{\xi}) = r(\xi_{32} \mid R'_{\xi}),$$
  

$$r(\xi_{19} \mid R'_{\xi}) = r(\xi_{22} \mid R'_{\xi}).$$

These equalities demonstrate that no vertex resolving set of cardinality three can resolve all vertices in  $G_s(Rb)$ , as shown in Figure 5. Therefore,

$$\xi \dim(G_s(Rb)) \ge 4. \tag{14}$$

We conclude by inequalities (13) and (14),

$$\xi \dim(G_s(Rb)) = 4.$$

This completes the proof.

**Theorem 3.8.** Let  $G_s(Tb)$  be a graph of Tucatinib. Then,  $\xi dim(G_s(Tb)) = 3$ .

*Proof.* Consider the connected graph  $G_s(Tb)$ , which has an vertex resolving set  $R_{\xi} = \{\xi_1, \xi_{26}, \xi_{33}\}$ , as illustrated in Figure 6. The vertex metric dimension of  $G_s(Tb)$  is 3.

To demonstrate this, we selected an vertex resolving set with a cardinality of 3 and defined it as follows,

$$r(\xi_j \mid R_{\xi}) = \{d(\xi_1), d(\xi_{26}), d(\xi_{33})\}.$$

To validate this statement, we present the following representations in Table 3 for further discussion.

Table 3: Resolving set of the molecular graph of Tucatinib with unique vertex representations.

j	$r(\xi_j R_{\xi}) = \{d(\xi_1), d(\xi_{26}), d(\xi_{33})\}$	j	$r(\xi_j R_{\xi}) = \{d(\xi_1), d(\xi_{26}), d(\xi_{33})\}$
1	(0, j+2, j+8)	20	$\left(\left(\frac{j}{2}\right), \left(\frac{j}{2}\right) - 7, \left(\frac{j}{2}\right) - 1\right)$
2	(j,6j+j,7+j)	21	(j-10, j-17, j-13)
3	(j-2,4j,6j)	22	$\left(j-10, \left(\frac{j}{22}\right)+2, \left(\frac{j}{2}\right)-4\right)$
4	(j-2,3j,4j+2)	23	(j-10, j-21, j-14)
5	(j-2, j+6, 3j+2)	24	$\left( \left( \frac{j}{2} \right) - 1, \left( \frac{j}{12} \right), \left( \frac{j}{2} \right) - 4 \right)$
6	(j-4, j+5, j+11)	25	$\left(\left(\frac{j}{5}\right) + 7, \left(\frac{j}{5}\right) - 4, \left(\frac{j}{5}\right) + 2\right)$
7	(j-4, j+3, j+9)	26	$\left(\left(\frac{j}{13}\right), 0, \left(\frac{j}{13}\right) + 6\right)$
8	(j-4, j+1j+7)	27	$\left(j-13,\left(\frac{j}{9}\right),\left(\frac{j}{9}\right)+2\right)$
9,10	(j-4, j-1, j+5)	28	$\left(j-13,\left(\frac{j}{4}\right)-3,\left(\frac{j}{4}\right)-3\right)$
11	(j-4, j-3, 3+j)	29	$\left(j - \frac{26}{2}, j - \frac{48}{2}, j - \frac{50}{2}\right)$
12, 13	(j-4, j-5, 1+j)	30	$\left(j - \frac{26}{2}, j - \frac{48}{2}, j - \frac{54}{2}\right)$
14	$\left(\left(\frac{j}{2}\right) + 3, \left(\frac{j}{2}\right), \left(\frac{j}{2}\right) + 6\right)$	31	$\left(j - \frac{26}{2}, j - \frac{48}{2}, j - \frac{58}{2}\right)$
15	$\left(\left(\frac{j}{3}\right) + 4, \left(\frac{j}{3}\right) + 1, \left(\frac{j}{3}\right) + 7\right)$	32	$\left(j - \frac{26}{2}, j - \frac{48}{2}, j - \frac{62}{2}\right)$
16	(j-8, j-11, j-5)	33	(j-14, j-25, 0)
17	$\left(j - \frac{20}{2}, j - \frac{22}{2}, j - \frac{10}{2}\right)$	34	(j-16, j-27, j-33)
18	$\left(j - \frac{24}{2}, j - \frac{22}{2}, j - \frac{10}{2}\right)$	35	(j-18, j-29, j-33)
19	(j-10, j-15, j-9)	36	(j-20, j-31, j-33)

It is evident from each vertices unique representation with  $R_{\xi}$  that  $R_{\xi}$  is an vertex resolving set of  $G_s(Tb)$ , which implies,

$$\xi \dim(G_s(Tb) \le 3. \tag{15}$$

Now, assume  $\xi \dim(G_s(Tb)) \geq 3$ . On contrary, suppose  $\xi \dim(G_s(Tb)) = 2$ . We consider,

**Case 1:** Let the path  $\xi_7 \to \xi_8 \to \xi_9$ ,  $\xi_{16} \to \xi_{19} \to \xi_{20}$ ,  $\xi_{23} \to \xi_{27} \to \xi_{28}$ ,  $\xi_{25} \to \xi_{26}$ , be a bridges.

Here,  $\xi_4$  and  $\xi_6$  are vertices from  $H_1$ , while  $\xi_{21}$  and  $\xi_{24}$  are vertices from  $H_2$ ,  $\xi_{32}$  and  $\xi_{33}$  are vertices from  $H_3$ , showing uniform representation. The same representation will appear at the following vertices if we choose an vertex resolving set from  $R'_{\xi} \subset \xi(H_1)$  with a cardinality of two,

$$r(\xi_4 \mid R_{\varepsilon}') = r(\xi_6 \mid R_{\varepsilon}').$$

It is impossible to resolve all the vertices.

**Case 2:** The same representation will appear at the following vertices if we choose an vertex resolving set from  $R'_{\xi} \subset \xi(H_2)$  with a cardinality of two,

$$r(\xi_{21} \mid R'_{\xi}) = r(\xi_{24} \mid R'_{\xi}),$$

and the same representation will appear at the following vertices if we choose an vertex resolving set from  $R'_{\xi} \subset \xi(H_3)$  with a cardinality of two,

$$r(\xi_{32} \mid R'_{\xi}) = r(\xi_{33} \mid R'_{\xi}).$$

**Case 3:** Even when considering an edge resolving set  $R'_{\xi}$  of cardinality two drawn from the union  $\xi(H_1) \cup \xi(H_2) \cup \xi(H_3)$ , The problem persists,

$$r(\xi_4 \mid R'_{\xi}) = r(\xi_6 \mid R'_{\xi}),$$
  

$$r(\xi_{21} \mid R'_{\xi}) = r(\xi_{24} \mid R'_{\xi}),$$
  

$$r(\xi_{32} \mid R'_{\xi}) = r(\xi_{33} \mid R'_{\xi}).$$

These equalities demonstrate that no vertex resolving set of cardinality two can resolve all vertices in  $G_s(Tb)$ , as shown in Figure 7. Therefore,

$$\xi \dim(G_s(Tb)) \ge 3. \tag{16}$$

We conclude by inequalities (15) and (16),

$$\mathcal{E}\dim(G_{\mathfrak{s}}(Tb))=3.$$

This completes the proof.

**Theorem 3.9.** Let  $G_s(Ob)$  be a graph of Olaparib. Then  $\xi dim(G_s(Ob)) = 3$ .

*Proof.* Consider the connected graph  $G_s(Ob)$ , which has an vertex resolving set  $R_{\xi} = \{\xi_7, \xi_{19}, \xi_{24}\}$ , as illustrated in Figure 8. The vertex metric dimension of  $G_s(Ob)$  is 3.

To demonstrate this, we selected an vertex resolving set with a cardinality of 3 and defined it as follows,

$$r(\xi_j \mid R_{\xi}) = \left\{ d(\xi_7), d(\xi_{19}), d(\xi_{24}) \right\}.$$

To validate this statement, we present the following representations in Table 4 for further discussion.

Table 4: Resolving set of the molecular graph of Olaparib with unique vertex representations.

j	$r(\xi_{j} R_{\xi}) = \left\{ d(\xi_{7}), d(\xi_{19}), d(\xi_{24}) \right\}$	j	$r(\xi_{j} R_{\xi}) = \left\{ d(\xi_{7}), d(\xi_{19}), d(\xi_{24}) \right\}$
1	(6-j,3(3)+j,7(2)+j)	19	(j-10,0,j-14)
2	$\left(2\left(j\right),4\left(j\right)+3,8\left(j\right)\right)$	20	$\left(\left(\frac{j}{2}\right), \left(\frac{j}{4}\right) - 4, \left(\frac{j}{4}\right) - 1\right)$
3	(j,7+j,5(j))	21	$\left(\left(\frac{j}{3}\right)+4,\left(\frac{j}{7}\right)-1,\left(\frac{j}{7}\right)\right)$
4	(j-2, j+5, 12+j)	22	(j-10, j-19, j-20)
5	(7 - j, j + 6, 3(j) + 1)	23	(j-10, j-19, j-22)
6	$\left(j - \frac{10}{2}, j + \frac{8}{2}, j + \frac{18}{2}\right)$	24	$\left(\left(\frac{j}{3}\right) + 5, \left(\frac{j}{4}\right) - 1, 0\right)$
7	$\left(j - \frac{14}{2}, j + \frac{4}{2}, 2\left(j\right)\right)$	25	(j-11, j-20, j-24)
8	(j-7,16-j,j+5)	26	$\left(\left(\frac{j}{2}\right), \left(\frac{j}{2}\right) - 9, \left(\frac{j}{2}\right) - 10\right)$
9, 10, 11	(j-7, j-2, j+3)	27	$\left(\left(\frac{j}{3}\right) + 1, \left(\frac{j}{3}\right) - 6, \left(\frac{j}{3}\right) - 5\right)$
12	$\left(\left(\frac{j}{4}\right), \left(\frac{j}{2}\right), \left(\frac{j}{4}\right) - 2\right)$	28	$\left(\left(\frac{j}{4}\right) + 2, \left(\frac{j}{4}\right) - 5, \left(\frac{j}{4}\right) - 2\right)$
13	$\left(j - \frac{18}{2}, j - \frac{16}{2}, j - \frac{6}{2}\right)$	29	(j-7(3), j-6(4), j-19)
14	(j-9, j-10, j-5)	30	(j-9(3), j-26, j-21)
15	(j-9, j-12, j-7)	31	(j-25, j-26, j-21)
16, 17	(j-9, j-14, j-9)	32	(j-27, j-26, j-21)
18	(j-10, j-17, j-12)		

It is evident from each vertices unique representation with  $R_{\xi}$  that  $R_{\xi}$  is an vertex resolving set of  $G_s(Ob)$ , which implies,

$$\xi \dim(G_s(Ob)) \le 3. \tag{17}$$

Now, assume  $\xi \dim(G_s(Ob)) \geq 3$ . On contrary, suppose  $\xi \dim(G_s(Ob)) = 2$ . We consider,

Case 1: Let the path  $\xi_9 \to \xi_{12} \to \xi_{13}$ ,  $\xi_{15} \to \xi_{16} \to \xi_{18}$ ,  $\xi_{16} \to \xi_{17}$ ,  $\xi_{21} \to \xi_{22} \to \xi_{23}$ ,  $\xi_{22} \to \xi_{26}$ , be a bridges. Here,  $\xi_5$  and  $\xi_7$  are vertices from  $H_1$ , while  $\xi_{17}$  and  $\xi_{18}$  are vertices from  $H_2$ ,  $\xi_{24}$  and  $\xi_{25}$  are vertices from  $H_3$ , showing uniform representation. The same representation will appear at the following vertices if we choose an vertex resolving set from  $R'_{\xi} \subset \xi(H_1)$  with a cardinality of two,

$$r(\xi_5 \mid R_{\varepsilon}') = r(\xi_7 \mid R_{\varepsilon}'),$$

it is impossible to resolve all the vertices.

**Case 2:** The same representation will appear at the following vertices if we choose an vertex resolving set from  $R'_{\xi} \subset \xi(H_2)$  with a cardinality of two,

$$r(\xi_{17} \mid R'_{\xi}) = r(\xi_{18} \mid R'_{\xi}),$$

and the same representation will appear at the following vertices if we choose an vertex resolving set from  $R'_{\xi} \subset \xi(H_3)$  with a cardinality of two,

$$r(\xi_{24} \mid R'_{\xi}) = r(\xi_{25} \mid R'_{\xi}).$$

**Case 3:** Even when considering an edge resolving set  $R'_{\xi}$  of cardinality two drawn from the union $\xi(H_1) \cup \xi(H_2) \cup \xi(H_3)$ , the problem persists,

$$r(\xi_5 \mid R'_{\xi}) = r(\xi_7 \mid R'_{\xi}),$$
  

$$r(\xi_{17} \mid R'_{\xi}) = r(\xi_{18} \mid R'_{\xi}),$$
  

$$r(\xi_{24} \mid R'_{\xi}) = r(\xi_{25} \mid R'_{\xi}).$$

These equalities demonstrate that no vertex resolving set of cardinality two can resolve all vertices in  $G_s(Ob)$ , as shown in Figure 9. Therefore,

$$\xi \dim(G_s(Ob)) \ge 3. \tag{18}$$

We conclude by inequalities (15) and (18),

$$\xi \dim(G_s(Ob) = 3.$$

This completes the proof.

**Theorem 3.10.** Let  $G_s(Ab)$  be a graph of Abemacicilb. Then,  $\xi dim(G_s(Ab)) = 3$ .

*Proof.* Consider the connected graph  $G_s(Ab)$ , which has an vertex resolving set  $R_{\xi} = \{\xi_5, \xi_{14}, \xi_{33}\}$ , as illustrated in Figure 10. The vertex metric dimension of  $G_s(Ab)$  is 3.

To demonstrate this, we selected an vertex resolving set with a cardinality of 3 and defined it as follows,

$$r(\xi_j \mid R_{\xi}) = \{d(\xi_5), d(\xi_{14}), d(\xi_{33})\}.$$

To validate this statement, we present the following representations in Table 5 for further discussion.

Table 5: Resolving set of the molecular graph of Abemaciclib with unique vertex representations.

	I		T
j	$r(\xi_j R_{\xi}) = \{d(\xi_5), d(\xi_{14}), d(\xi_{33})\}$	j	$r(\xi_j R_{\xi}) = \{d(\xi_5), d(\xi_{14}), d(\xi_{33})\}$
1, 2, 3, 4, 5	(5-j, 10-j, 21-j)	22	$\left(j-12,\left(\frac{j}{2}\right)-6,\left(\frac{j}{2}\right)-5\right)$
6	(j-5, 10-j, 21-j)	23	(j-12,4,7)
7	(j-5, j-2, 2j+2)	24	$\left(\left(\frac{j}{2}\right) - 1, \left(\frac{j}{2}\right) - 6, \left(\frac{j}{2}\right) - 7\right)$
8	(j-5, j-2, 2j+1)	25	$\left(\left(\frac{j}{5}\right) + 7, \left(\frac{j}{5}\right) + 2, \left(\frac{j}{5}\right) + 1\right)$
9	(j-7, j-6, j+5)	26	$\left(\left(\frac{j}{2}\right), \left(\frac{j}{2}\right) - 5, \left(\frac{j}{2}\right) - 8\right)$
10	(j-7, j-8, j+3)	27	$\left(\left(\frac{j}{3}\right) + 5, \left(\frac{j}{3}\right), \left(\frac{j}{3}\right) - 3\right)$
11	(j-7, j-8, j+1)	28	$\left(\left(\frac{j}{2}\right), \left(\frac{j}{4}\right) + 2, \left(\frac{j}{7}\right)\right)$
12	$\left(j - \frac{14}{2}, j - \frac{20}{2}, j - \frac{2}{2}\right)$	29	(j-17, j-22, j-25)
13	$\left(j - \frac{14}{2}, j - \frac{24}{2}, j - \frac{6}{2}\right)$	30	(j-17, j-22, j-27)
14	$\left(j - \frac{18}{2}, j - \frac{28}{2}, j - \frac{6}{2}\right)$	31	(j-17, j-22, j-29)
15	(j-11, 16-j, j-6)	32	(j-17, j-22, j-31)
16	(j-9, j-12, j-7)	33	(j-17, j-22, j-33)
17	(j-9, j-13, j-9)	34	(j-18, j-23, j-32)
18	(j-9, j-14, j-9)	35	(j-19, j-24, j-31)
19	(j-9, j-15, j-11)	36	(j-21, j-26, j-33)
20	(j-9, j-14, j-13)	37	(j-21, j-27, j-33)
21	$\left(\left(\frac{j}{3}\right) + 5, \left(\frac{j}{3}\right), \left(\frac{j}{3}\right) - 1\right)$		

It is evident from each vertices unique representation with  $R_{\xi}$  that  $R_{\xi}$  is an vertex resolving set of  $G_s(Ab)$ , which implies,

$$\xi \dim(G_s(Ab)) \le 3. \tag{19}$$

Now, assume  $\xi \dim(G_s(Ab)) \geq 3$ . On contrary, suppose  $\xi \dim(G_s(Ab)) = 2$ . We consider,

**Case 1:** Let the path  $\xi_7 \to \xi_8 \to \xi_9$ ,  $\xi_{16} \to \xi_{19} \to \xi_{20}$ ,  $\xi_{23} \to \xi_{27} \to \xi_{28}$ ,  $\xi_{25} \to \xi_{26}$ , be a bridges. Here,  $\xi_4$  and  $\xi_6$  are vertices from  $H_1$ , while  $\xi_{21}$  and  $\xi_{224}$  are vertices from  $H_2$ ,  $\xi_{32}$  and  $\xi_{33}$ 

are vertices from  $H_3$ , showing uniform representation. The same representation will appear at the following vertices if we choose an vertex resolving set from  $R'_{\xi} \subset \xi(H_1)$  with a cardinality of two,

$$r(\xi_4 \mid R'_{\xi}) = r(\xi_6 \mid R'_{\xi}).$$

It is impossible to resolve all the vertices.

**Case 2:** The same representation will appear at the following vertices if we choose an vertex resolving set from  $R'_{\xi} \subset \xi(H_2)$  with a cardinality of two,

$$r(\xi_{21} \mid R'_{\xi}) = r(\xi_{24} \mid R'_{\xi}),$$

and the same representation will appear at the following vertices if we choose an vertex resolving set from  $R'_{\xi} \subset \xi(H_3)$  with a cardinality of two,

$$r(\xi_{32} \mid R'_{\varepsilon}) = r(\xi_{33} \mid R'_{\varepsilon}).$$

**Case 3:** Even when considering an edge resolving set  $R'_{\xi}$  of cardinality three drawn from the union  $\xi(H_1) \cup \xi(H_2) \cup \xi(H_3)$ , the proplem persists,

$$r(\xi_4 \mid R'_{\xi}) = r(\xi_6 \mid R'_{\xi}),$$
  

$$r(\xi_{21} \mid R'_{\xi}) = r(\xi_{24} \mid R'_{\xi}),$$
  

$$r(\xi_{32} \mid R'_{\xi}) = r(\xi_{33} \mid R'_{\xi}).$$

These equalities demonstrate that no vertex resolving set of cardinality two can resolve all vertices in  $G_s(Ab)$ , as shown in Figure 11. Therefore,

$$\xi \dim(G_s(Ab)) \ge 3. \tag{20}$$

We conclude by inequalities (19) and (20),

$$\xi \dim(G_s(Ab)) = 3.$$

This completes the proof.

#### 4 Conclusion

This study addresses the structures of different cancer drugs and computes their vertex and edge metric dimensions, resolving a collection of molecular graphs of drugs used in breast cancer therapy. This paper provided a brief overview of some molecular structures using the metric of vertices and edges in chemical graph theory. Key nodes, such as proteins, genes, or molecular targets, may be discovered in the biological network of breast cancer by applying the metric dimension idea. The structure's pivotal points have a major impact on medication resistance or the advancement of cancer. By concentrating on these nodes, medicines that are more individualized and effective may be developed. Moreover, Table 6 provides a summary of the key findings.

Table 6: Summary of the result.

Drugs	Vertex Metric Dimension	Edge Metric Dimension
$G_s(Te)$	4	3
$G_s(Rb)$	4	3
$G_s(Tb)$	3	3
$G_s(Ob)$	3	3
$G_s(Ab)$	3	3

#### Open Problem

- Problem 1: Compute the mixed metric dimension for the molecular graph of breast cancer drugs.
- Problem 2: Compute the fault-tolerant metric dimension for the molecular graph of breast cancer drugs.

**Acknowledgement** The authors would like to take this opportunity to thank the management of Vellore Institute of Technology, Vellore, Tamil Nadu, India, for providing the necessary facilities and encouragement to carry out this work.

**Conflicts of Interest** The authors declare no conflict of interest that could have affected the research and conclusions presented in this paper.

#### References

- [1] A. Ahmad, A. N. A. Koam, M. Azeem, I. Masmali & R. Alharbi (2024). Edge based metric dimension of various coffee compounds. *PLOS One*, 19(4), Article ID: e0294932. https://doi.org/10.1371/journal.pone.0294932.
- [2] A. Ahmad, A. N. A. Koam, M. H. F. Siddiqui & M. Azeem (2022). Resolvability of the starphene structure and applications in electronics. *Ain Shams Engineering Journal*, 13(2), Article ID: 101587. https://doi.org/10.1016/j.asej.2021.09.014.
- [3] S. Ali, R. Ismail, F. J. H. Campena, H. Karamti & M. U. Ghani (2023). On rotationally symmetrical planar networks and their local fractional metric dimension. *Symmetry*, 15(2), Article ID: 530. https://doi.org/10.3390/sym15020530.
- [4] U. Farooq, F. Chudhary, D. Afzal & W. Abbas. Fault-tolerant metric dimension (FTMD) of M-polynomial of zigzag edge coronoid fused by starphene. Preprint 2023. https://doi.org/10.21203/rs.3.rs-3783303/v1.
- [5] K. J. Gowtham & M. N. Husin (2023). A study of families of bistar and corona product of graph: Reverse topological indices. *Malaysian Journal of Mathematical Sciences*, 17(4), 575–586. https://doi.org/10.47836/mjms.17.4.04.
- [6] F. Harary & R. A. Melter (1976). On the metric dimension of a graph. *Ars Combinatoria*, 1976(2), 191–195.
- [7] Q. Huang, A. Khalil, D. A. Ali, A. Ahmad, R. Luo & M. Azeem (2022). Breast cancer chemical structures and their partition resolvability. *Mathematical Biosciences and Engineering*, 20(2), 3838–3853. https://doi.org/10.3934/mbe.2023180.
- [8] M. Imran, M. K. Siddiqui & R. Naeem (2018). On the metric dimension of generalized petersen multigraphs. *IEEE Access*, 6, 74328–74338. https://doi.org/10.1109/ACCESS.2018.2883556.
- [9] G. Ismail, N. H. Sarmin & N. I. Alimon (2025). The distance-based topological indices of the zero divisor graph for some commutative rings with the calculator app. *Malaysian Journal of Mathematical Sciences*, 19(1), 207–222. https://doi.org/10.47836/mjms.19.1.11.

- [10] S. Khuller, B. Raghavachari & A. Rosenfeld (1996). Landmarks in graphs. *Discrete Applied Mathematics*, 70(3), 217–229. https://doi.org/10.1016/0166-218X(95)00106-2.
- [11] A. N. A. Koam, A. Ahmad, M. E. Abdelhag & M. Azeem (2021). Metric and fault-tolerant metric dimension of hollow coronoid. *IEEE Access*, *9*, 81527–81534. https://doi.org/10.1109/ACCESS.2021.3085584.
- [12] J. B. Liu, S. K. Sharma, V. K. Bhat & H. Raza (2023). Multiset and mixed metric dimension for starphene and zigzag-edge coronoid. *Polycyclic Aromatic Compounds*, 43(1), 190–204. https://doi.org/10.1080/10406638.2021.2019066.
- [13] J. Lv, X. Lv, R. Nasir & Z. Zahids (2021). The edge version of metric dimension for the family of circulant graphs  $C_n(1,2)$ . *IEEE Access*, 9, 78165–78173. https://doi.org/10.1109/ACCESS. 2021.3083182.
- [14] M. F. Nadeem, M. Azeem & A. Khalil (2021). The locating number of hexagonal Möbius ladder network. *Journal of Applied Mathematics and Computing*, 66, 149–165. https://doi.org/10.1007/s12190-020-01430-8.
- [15] M. F. Nadeem, M. Hassan, M. Azeem, S. Ud-Din Khan, M. R. Shaik, M. A. F. Sharaf, A. Abdelgawad & E. M. Awwad (2021). Application of resolvability technique to investigate the different polyphenyl structures for polymer industry. *Journal of Chemistry*, 2021(1), Article ID: 6633227. https://doi.org/10.1155/2021/6633227.
- [16] R. Nawaz, M. K. Jamil & M. Azeem (2024). Edge-based metric resolvability of anti-depression molecular structures and its application. *Results in Chemistry*, 7, 101458. https://doi.org/10.1016/j.rechem.2024.101458.
- [17] R. Nithya Raj, R. Sundara Rajan, I. Rajasingh & I. N. N. Cangul (2024). Metric dimension for line graph of some chemical structures. *Iranian Journal of Mathematical Chemistry*, 15(4), 269–282. https://doi.org/10.22052/ijmc.2024.254131.1817.
- [18] C. J. Rayer & R. S. Jeyaraj (2023). Applications on topological indices of zero-divisor graph associated with commutative rings. *Symmetry*, 15(2), Article ID: 335. https://doi.org/10.3390/sym15020335.
- [19] C. J. Rayer & R. S. Jeyaraj (2023). Graph energy and topological descriptors of zero divisor graph associated with commutative ring. *Journal of Applied Mathematics and Computing*, 69(3), 2641–2656. https://doi.org/10.1007/s12190-023-01837-z.
- [20] Z. Raza & M. S. Bataineh (2021). The comparative analysis of metric and edge metric dimension of some subdivisions of the wheel graph. *Asian-European Journal of Mathematics*, 14(4), Article ID: 2150062. https://doi.org/10.1142/S1793557121500625.
- [21] B. Rohr, H. S. Stein, D. Guevarra, Y. Wang, J. A. Haber, M. Aykol, S. K. Suram & J. M. Gregoire (2020). Benchmarking the acceleration of materials discovery by sequential learning. *Chemical Science*, 11(10), 2696–2706. https://doi.org/10.1039/C9SC05999G.
- [22] A. Sebő & E. Tannier (2004). On metric generators of graphs. *Mathematics of Operations Research*, 29(2), 383–393. https://doi.org/10.1287/moor.1030.0070.
- [23] K. Sharma, V. K. Bhat & S. K. Sharma (2022). Edge metric dimension and edge basis of one-heptagonal carbon nanocone networks. *IEEE Access*, 10, 29558–29566. https://doi.org/10.1109/ACCESS.2022.3158982.
- [24] S. K. Sharma, V. K. Bhat, H. Raza & K. Sharma. Metric and edge metric dimension of zigzag edge coronoid fused with starphene. arXiv preprint arXiv:2107.14484 2021. https://doi.org/10.48550/arXiv.2107.14484.

- [25] S. K. Sharma, V. K. Bhat, H. Raza & S. Sharma (2022). On mixed metric dimension of polycyclic aromatic hydrocarbon networks. *Chemical Papers*, 76(7), 4115–4128. https://doi.org/10.1007/s11696-022-02151-x.
- [26] H. M. A. Siddiqui, S. Hayat, A. Khan, M. Imran, A. Razzaq & J. B. Liu (2019). Resolvability and fault-tolerant resolvability structures of convex polytopes. *Theoretical Computer Science*, 796, 114–128. https://doi.org/10.1016/j.tcs.2019.08.032.
- [27] M. Singh, S. K. Sharma & V. K. Bhat (2023). On mixed metric dimension of crystal cubic carbon structure. *Journal of Mathematical Chemistry*, 61(10), 2079–2097. https://doi.org/10.1007/s10910-023-01507-2.
- [28] P. J. Slater (1975). Leaves of trees. Congressus Numerantium, 14, 549–559.